Article:
Menon, M. orcid.org/0000-0001-5665-7464, Smalley, A., Geraki, K. et al. (2 more authors) (2025) A comparison of micronutrient elements in cooked white, brown and parboiled rice using synchrotron micro-X-ray fluorescence imaging. Food Chemistry. 146421-. ISSN: 0308-8146

https://doi.org/10.1016/j.foodchem.2025.146421

Food Chemistry

A comparison of micronutrient elements in cooked white, brown and parboiled rice using synchrotron micro-X-ray fluorescence imaging

--Manuscript Draft--

Manuscript Number:	FOODCHEM-D-25-04585R2
Article Type:	Research Article (max 7,500 words)
Keywords:	Rice, nutrient elements, X-ray fluorescence, Synchrotron, Spectroscopy
Corresponding Author:	Manoj Menon, Ph.D. University of Sheffield Sheffield, UNITED KINGDOM
First Author:	Manoj Menon, Ph.D.
Order of Authors:	Manoj Menon, Ph.D.
	Alan Smalley, PhD(Current)
	Kalotina Geraki, PhD
	Viren Ranawana, PhD
Abstract:	Rice is a staple food for over half the world's population. This study uniquely investigates the spatial distribution of key micronutrients (Cu, Mn, Fe, Zn) in cooked brown, white, and parboiled rice using Synchrotron Micro-X-ray Fluorescence (sXRF) for the first time. Complementary analysis with Inductively Coupled Plasma Mass Spectrometry (ICP-MS) validates bulk elemental concentrations. Results from this dual-approach study reveal significantly higher micronutrient concentrations in brown rice compared to white or parboiled rice, with nutrients predominantly localised in the peripheral layers and minimal presence in the endosperm. Notably, sXRF imaging identified nutrient-rich pockets within the grain periphery, offering new perspectives on nutrient distribution beyond peripheral accumulation. Additional insights include the impact of rice section thickness (50 and 150 μm) and beam dwell times (0.5 and 30s) on sXRF sensitivity and resolution, highlighting trade-offs in detection capabilities, advancing our understanding of micronutrient localisation in cooked rice.

Highlights

-Cooked brown, white and parboiled rice types were mapped for micronutrients

- Elemental maps of Cu, Mn, Fe and Zn were produced using sXRF

- Concentration of these elements was in the order: Brown > white > parboiled

- Very good agreement between sXRF and ICP-MS measurements

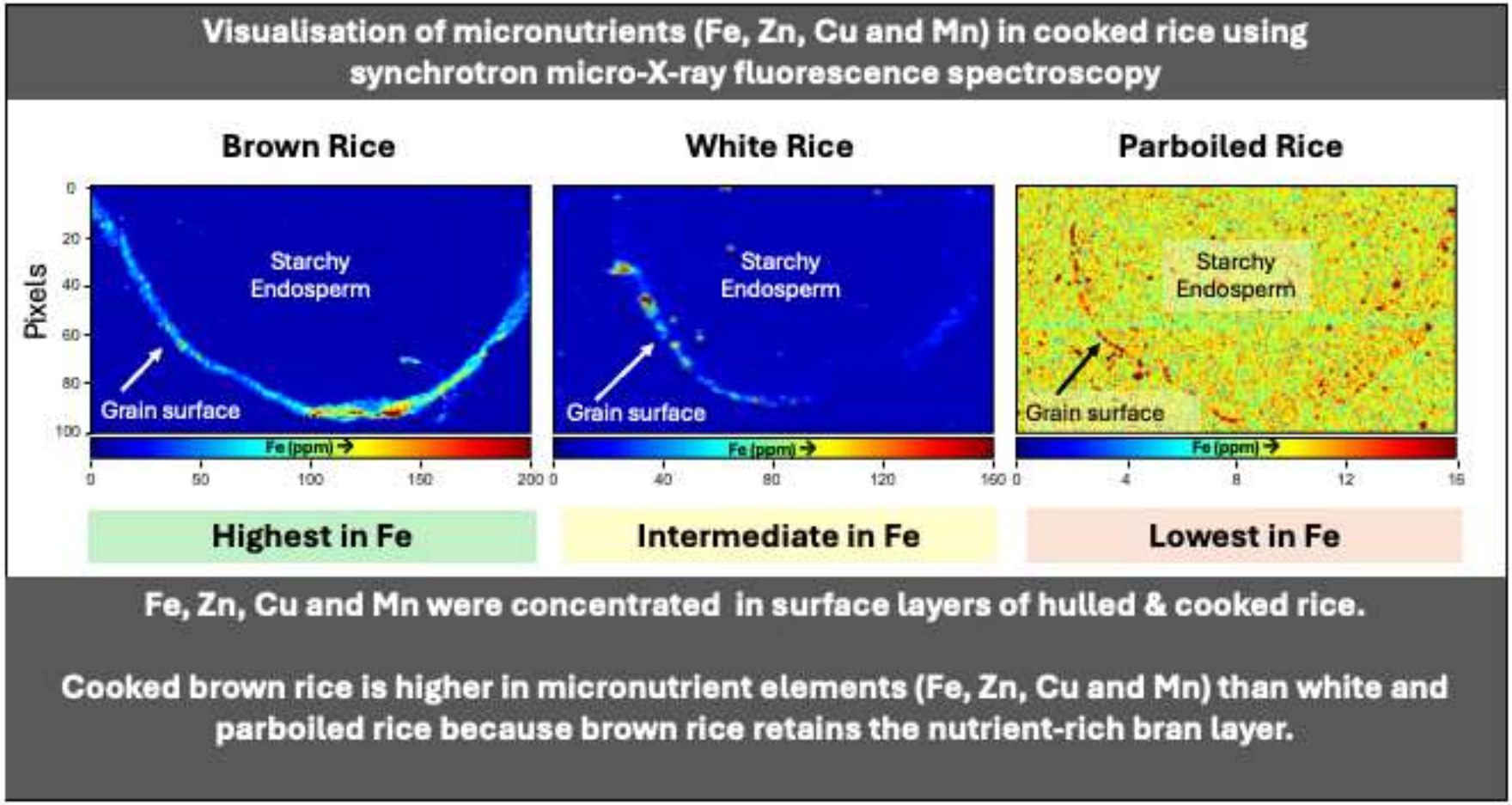

A comparison of micronutrient elements in cooked white, brown and parboiled rice using synchrotron micro-X-ray fluorescence imaging

Manoj Menon[1*], Alan Smalley[1], Kalotina Geraki[2], Masoud Babaei[3], Viren Ranawana[1]

[1] The University of Sheffield, Western Bank, Sheffield United Kingdom S102TN

[2] Diamond Light Source, Harwell Science and Innovation Campus, Fermi Ave, Didcot OX11 0DE

[3]University of Manchester, Oxford Rd, Manchester M13 9PL

*Corresponding author

m.menon@sheffield.ac.uk

Abstract

Rice is a staple food for over half the world's population. This study uniquely investigates the spatial distribution of key micronutrients (Cu, Mn, Fe, Zn) in cooked brown, white, and parboiled rice using Synchrotron Micro-X-ray Fluorescence (sXRF) for the first time. Complementary analysis with Inductively Coupled Plasma Mass Spectrometry (ICP-MS) validates bulk elemental concentrations. Results from this dual-approach study reveal significantly higher micronutrient concentrations in brown rice compared to white or parboiled rice, with nutrients predominantly localised in the peripheral layers and minimal presence in the endosperm. Notably, sXRF imaging identified nutrient-rich pockets within the grain periphery, offering new perspectives on nutrient distribution beyond peripheral accumulation. Additional insights include the impact of rice section thickness (50 and 150 µm) and beam dwell times (0.5 and 30s) on sXRF sensitivity and resolution, highlighting trade-offs in detection capabilities, advancing our understanding of micronutrient localisation in cooked rice.

Keywords: Rice, Nutrient elements, X-ray fluorescence, Synchrotron, Spectroscopy

1. Introduction

Rice (*Oryza sativa* L.) supplies up to 70% of the energy requirements for more than half the global population (Bin Rahman & Zhang, 2023; International Rice Research Institute, 2013). Currently, global rice production is ~540 million tonnes, and 90% of it is produced and consumed in Asia (FAO, 2025; OECD, 2015) as white (polished) or parboiled white rice. Parboiled rice is produced by soaking, steaming, and drying the harvested grains before milling and polishing (Balbinoti et al., 2018). On the other hand, brown rice – consisting of the whole (unpolished) grain, which includes the bran layer – is nutritionally superior (Menon et al., 2024; Saleh et al., 2019) and has a lower Glycaemic index than white rice (Chang et al., 2014; Kaur et al., 2016).

The nutrient element concentration of rice varies depending on the rice type (Antoine et al., 2012; Menon et al., 2022; Pinto et al., 2016) with brown rice (raw or cooked) shown to be richer in nutrient elements including P, K, Mg, K, Fe, Zn and Mn when compared to white or parboiled rice. Cooking can significantly affect the stability and distribution of trace elements within the grain due to water ingress, grain rupture and gelatinisation. Studies have reported changes in total elemental concentrations in rice, influenced by rice type and cooking method, primarily determined by Inductively Coupled Plasma Mass Spectrometry (ICP-MS) (Gray et al., 2015; Menon et al., 2021, 2024). These studies showed a post-cooking loss of nutrients such as P, K, Mg, Fe, Mn, Cu and Mo, along with toxic elements such as As, depending on the cooking method and rice type used. Specifically, studies also show that absorption-based cooking methods minimise the loss of nutrients when compared with excess water-based cooking methods because, in the former, no water is discarded during

or after the cooking process. Also, these studies consistently showed better retention of nutrient elements in brown rice compared to white or parboiled rice.

Wet lab analysis methods, such as ICP-MS, can be used to quantify total nutrient element concentrations in homogenised (powdered and acid-digested) rice samples, but these methods do not provide information about the distribution of elements within the grain. Knowing the spatial distribution of micronutrients in rice is crucial for tackling malnutrition (Welch & Graham, 2004, 2005). This is especially pertinent in regions that depend heavily on polished white rice (Dipti et al., 2012) as the milling process removes the nutrient-rich bran layer and germ, significantly reducing essential nutrients such as iron (Fe) and zinc (Zn). Identifying nutrient locations within the grain (e.g., aleurone layer, the embryo, starchy endosperm) could support biofortification efforts to enhance micronutrient content in the edible portion (White & Broadley, 2009). This knowledge could also be applied to inform crop and yield improvement strategies, such as identifying rice genotypes that efficiently take up and translocate micronutrients to the grain or optimising agronomic practices for better nutrient quality (Cakmak, 2008).

Furthermore, the bioavailability of nutrients is influenced by both their location, chemical form and the presence of antinutrients such as phytates. Therefore, understanding the spatial distribution of nutrients enhances our comprehension of the absorption kinetics of trace elements (Goff, 2018). Specifically, the proportions of trace elements absorbed in the duodenum and ileum differ from those absorbed in the colon. Nutrients situated more superficially or migrated into the endosperm are more likely to be absorbed in the small intestine, whereas those retained in the bran after cooking are more likely to be absorbed in the colon. Research indicates that bran undergoes fermentation and breakdown in the colon, supporting the argument

that phytate-bound trace elements within bran are released during this process and subsequently absorbed (Nealon et al., 2019; Yilmaz & Li, 2018).

Additionally, rice can accumulate toxic elements like As and Cd, posing food safety risks (Menon et al., 2020; Shi et al., 2020; Williams et al., 2007). Identifying the spatial distribution of these contaminants within the grain helps in developing strategies to mitigate risks and breed rice varieties that either exclude or compartmentalise these toxic elements in non-edible or discarded parts.

Qualitative and quantitative high-resolution imaging methods can be used to map nutrient element spatial distributions, provided such elements are present in sufficient (i.e. detectable) quantities. Unlike wet lab methods, these imaging techniques can be performed with minimal or no damage to the original sample. For instance, previous researchers have used nanoscale secondary ion mass spectroscopy (nano SIMS) to analyse cereal grains (Moore et al., 2010; Wang et al., 2022). In contrast, others have used synchrotron-based micro X-ray fluorescence (sXRF) in rice, but these studies were limited to uncooked, unhusked or unpolished rice grains (Limmer et al., 2023; Lombi et al., 2009; Meharg et al., 2008; Mihucz et al., 2010; Oli et al., 2016). A significant gap, therefore, exists in the understanding of nutrient element distributions within cooked rice grains. Specifically, no studies have employed synchrotron-based X-ray fluorescence (sXRF) to investigate elemental distributions in cooked rice. This method can also provide detailed insights into the effects of nutrient diffusion during parboiling or cooking.

Therefore, this study aims to bridge this gap by applying sXRF to analyse different rice types, namely brown, white, and parboiled rice, for the first time. The focus is on

essential nutrient elements—iron (Fe), zinc (Zn), copper (Cu), and manganese (Mn)—due to their critical roles in public health. A key advantage of sXRF is its capability to identify nutrient element hotspots within samples, offering detailed spatial distribution insights. To achieve accurate and reliable results, the study will also address methodological optimisations, such as determining suitable sample thickness and beam dwell time, and will validate findings through comparison with traditional wet lab-based methods like ICP-MS. The primary objectives of this study were:

1. To investigate the spatial distribution patterns of nutrient elements (Fe, Zn, Cu, Mn) within cooked rice grains, whilst exploring sample thickness and beam dwell time.
2. To compare the nutrient element abundances across different rice types (brown, white, and parboiled) using both sXRF and ICP-MS analyses.

2. **Methods**

2.1 Sample preparation

Since rice is not cultivated in the UK, we sourced three types of Basmati rice (brown, white, and parboiled; non-organic, origin-unspecified) from a UK supermarket (Morrisons). We acknowledge that nutrient concentrations will depend on several factors, such as the origin and agronomic practices. However, our earlier research, conducted with a substantially larger sample set (54 rice products) available in the UK, revealed minimal variation in nutrient elements within each rice type, with significant differences in nutrient elements between different rice types, such as white and brown (Menon et al., 2022).

142 The method of cooking plays a crucial role in determining the concentration of
143 minerals in cooked rice. Considering the wide range of available techniques, we
144 employed our previously validated cooking protocol (Menon et al., 2021, 2024),
145 which has proven effective in reducing toxic elements such as arsenic, while
146 maintaining a range of essential macro- and micronutrients. This protocol
147 distinctively integrates both the absorption and the excess water cooking methods.
148 In this method, rice was first boiled for 5 min in tap water using an initial rice-to-water
149 volumetric ratio of 1:4 (note that elemental composition data for the tap water is
150 provided in Supplementary Material 1). This ratio equated to 20±0.25mL (17±0.1g) of
151 rice and 80mL of tap water. After 5 min, the samples were drained to remove the
152 excess water, and a fresh volume of tap water (50mL) was added, following which
153 the samples were cooked until tender and the water fully absorbed (approx. 12-20
154 min, depending on the type of rice). After cooking, the samples were cooled, and
155 several firm grains were separated from the cooked mass and transferred to a Petri
156 dish for thin sectioning. The remaining rice was dried and powdered using a ceramic
157 ball mill to produce a homogenous sample for micronutrient element analysis
158 (section 2.2) in triplicate.
159
160 The cooked rice grains were air-dried in Petri dishes overnight to partially firm up
161 before transferring into an OCT (Optimal Cutting Temperature) medium (Agar
162 Scientific, UK), then flash-frozen using liquid nitrogen. Sections at thicknesses of
163 50,100, and 150 µm were taken from the middle of the grain using a Leica CM3050S
164 cryostat. The temperature in the microtome chamber was -20°C. The sections were
165 transferred onto 1-mm thick high-purity fluorescence-free fused quartz microscope
166 slides (75 x 25mm, UQG Optics Ltd, United Kingdom). A circular piece of Kapton^{TM}

tape (polyimide film, free from traces of the elements studied here) was placed over the thin section to secure it on the slide. Multiple sections were prepared for imaging, as shown in Fig. 1. Brown rice cross-sections were semi-circular, while white and parboiled rice were nearly circular when viewed under an optical microscope. Our focus was to acquire as many reproducible transect scans as possible, focusing on the peripheral regions of the grain where nutrient concentrations are highest, rather than scanning the entire grain, which predominantly contains the starchy interior (see Section 2.3).

2.2 Micronutrient element analysis in rice using ICP-MS

For elemental analysis, triplicate samples were processed at the School of Bioscience, University of Nottingham, UK, following the protocol described in our previous publications (Mauer et al., 2024; Menon et al., 2024). Briefly, approximately 0.2 g (dry weight) of powdered sample was microwave-digested in 6 mL HNO_3 (Primar grade, Fisher Scientific), using perfluoro-alkoxy (PFA) vessels (Multiwave; Anton Paar GmbH). The digested samples were diluted to 20 mL total volume in Milli-Q water (18.2 MΩ cm). This was then subsampled and further diluted 1-in-10 using Milli-Q water. Analysis of diluted solutions was undertaken by ICP-MS (Thermo-Fisher Scientific iCAP-Q and iCAP-TQ). A Claritas-PPT grade multi-element calibration standard was used, which included the four elements of interest for this study (Fe, Zn, Cu and Mn) at concentrations of 0, 20, 40 and 100 µg L^{-1}. The matrices used for internal standards, calibration standards and sample diluents was 2% HNO_3 with 4% methanol (to enhance ionisation of some elements). To quantify recovery in the digest and analysis procedures, a National Institute of Standards and Technology (NIST)-certified reference material (NIST 1568b rice flour) was analysed

192 in triplicate, giving recoveries for Fe, Zn, Cu and Mn of 89, 93, 96 and 95%,
193 respectively, with relative standard deviation (RSD) values of 0.62, 0.90, 1.40 and
194 0.35%, respectively. Additional ICP-MS settings, along with calibration data for the
195 elements of interest, plus LoD and LoQ values, are provided in Supplementary
196 Material 2.
197
198 2.3 Elemental Imaging
199 Imaging experiments were conducted at the UK National Synchrotron (Diamond
200 Light Source, Didcot OX11 0DE) using I18, the microfocus spectroscopy beamline.
201 I18 is optimised for performing high-resolution sXRF analysis with relatively high
202 sensitivity for dilute elements (Adams, 2003). It uses a double-crystal
203 monochromator to tune the energy of the primary beam and a pair of Kirkpatrick-
204 Baez (KB) focusing mirrors that allow beam size adjustment to match experimental
205 requirements (Mosselmans et al., 2009). It is important to note that sXRF facilities
206 are expensive and rare, and are therefore in high demand. Researcher access is
207 typically limited to short time windows, which restricts the number of samples that
208 can be realistically evaluated.
209
210 In the first few hours, preliminary test scans were conducted to determine the
211 scanning parameters, such as spot size, dwell time, excitation energy and detector
212 distance. Based on this, the beamline spot (i.e. pixel resolution) was set at 10x10
213 μm^2 and the energy at 12.5 keV. A Vortex silicon drift detector was used to collect
214 the fluorescence signal from the samples. The dwell time was either 0.5s or 30s per
215 point, depending on the size of the total area scanned.
216

An optical microscope was used to select the thin sections for their structural integrity prior to imaging. Scans of 50 µm-thick samples and 150 µm-thick samples were made at 0.5s dwell time, and additional scans focusing on the grain edges were made at 30s dwell time. These three transect scans aimed to generate reproducible elemental maps within the allocated beam time. The two different thicknesses were used to explore what worked best in terms of both sensitivity and resolution. The duration of each scan was 4-10 hours, depending on the acquisition time and ROI (region of interest) selected. The ROI chosen for each scan was based on sample shape, which varied between the cross-sections.

2.4 Data processing and analysis:

The raw spectra obtained from the beamline were processed with the software package PyMca (Solé et al., 2007), which was developed at the European Synchrotron Radiation Facility for the qualitative and quantitative analysis of sXRF maps. The software implements peak deconvolution and removal of the background continuum, allowing the user to fine-tune the configuration parameters for optimum fit of their data. An example of a raw spectrum and the fitted one in PyMca is shown in Fig. 2.

A reference material developed for the quantification of elements via sXRF imaging, was used to estimate the concentrations of the elements of interest. The reference material, from AXO (Dresden), comprises nm-thick layers of 6 metals (including Fe and Cu), and the manufacturers provide accurately measured mass deposition of each element. The reference material is measured under the same conditions as the samples, and this, in conjunction with modelling of the main experimental conditions (incoming photon energy, detector material, detector window, active area and

242 distance from sample), is used to calculate the photon flux on the sample. All this
243 forms a configuration which, when applied to the sample measurements (their matrix
244 and thickness also considered), allows the conversion of elemental peak counts to
245 concentration values (ppm). This resulted in separate elemental concentration maps
246 from which TIFF images were produced. The original TIFF images were displayed
247 with MATLAB with a suitable scale range for optimum visualisation without any
248 image modifications or processing. A final set of images for Cu, Mn, Fe and Zn was
249 selected for this paper.
250 It is not possible to give an across-the-board reference for the sensitivity of the
251 microprobe, as limits depend heavily on a particular set-up, which is fine-tuned for
252 each experiment. This is on top of the known dependence on sample matrix,
253 thickness, and elements measured. The ball-park approach is that the sensitivity of
254 such synchrotron probes is at least single unit ppm levels.

255 **3. Results and discussion**

256 *3.1 Micronutrient elements concentrations in rice using ICP-MS.*

257 The concentration of the elements of interest in this study is presented in Fig. 3. The
258 mean Mn concentration was highest in brown rice (19.61 mg kg^{-1}), followed by white
259 (7.68 mg kg^{-1}) and parboiled rice (4.22 mg kg^{-1}). Fe concentration in brown rice
260 (15.39 mg kg^{-1}) was 4-5 times higher than in white or parboiled rice, whereas Cu
261 concentrations of the three rice types were very similar, ranging from 1.99 mg kg^{-1} in
262 parboiled rice to 2.43 mg kg^{-1} in white rice and 2.81 mg kg^{-1} in brown rice. The
263 concentration of Zn was highest in brown (18.61 mg kg^{-1}), followed by white rice
264 (15.92 mg kg^{-1}) and parboiled rice (7.45 mg kg^{-1}). Note that for each set of triplicates,
265 RSD values were <5%, except for Fe in white and parboiled rice, where the RSD
266 values were 20.6% and 9.0%, respectively. Samples were corrected against blanks,

all of which showed negligible contamination. The one-way ANOVA revealed a statistically significant effect ($p < 0.0001$) of rice types on all the elements studied. Subsequent post-hoc Dunnett's multiple comparison test indicated significant differences between white and brown rice for Cu ($p = 0.0004$), Mn ($p < 0.0001$), Fe ($p < 0.0001$), and Zn ($p = 0.0005$). Similarly, comparisons between white and parboiled rice showed statistically significant differences for Cu ($p = 0.0001$), Mn ($p < 0.0001$), and Zn ($p < 0.0001$), while the difference for Fe was not significant ($p = 0.1052$).

These results are consistent with our previous study, which showed that Fe and Zn concentrations were much higher in cooked brown rice than in the other rice types, whereas Cu concentrations were comparable in all three rice types (Menon et al., 2024). In studies where raw/uncooked rice types were compared for nutrient elements, brown rice was superior to other rice types, such as white or parboiled. When we compared (Menon et al., 2022) raw white ($n = 36$) and brown rice ($n = 13$) from the UK market, we found that Fe, Mn and Zn concentrations in the latter were significantly higher than in white rice. Similar nutrient trends across these rice types were observed in a previous study (Pinto et al., 2016), which compared uncooked brown, parboiled and white rice sold in Spanish and Portuguese markets. Conversely, a study on rice sold in Jamaican markets did find that Cu, Zn and Mn were higher in raw brown rice than in white rice, whereas Fe concentrations were comparable in both types (Antoine et al., 2012). However, although broad trends do show some variation, the composition results presented in this study are consistent with the majority of previous studies, which show that brown rice is nutritionally superior to white rice (including for micronutrients) (Wu et al., 2023). Micronutrient deficiencies remain a hallmark of malnutrition and hidden hunger in the global south

(Stevens et al., 2022), where rice (in its white rice form) is the main staple and source of energy (Bin Rahman & Zhang, 2023). Therefore, increasing brown rice consumption can potentially improve micronutrient status in at-risk populations.

A limitation to micronutrient bioavailability from brown rice is the presence of phytic acid, predominantly within the aleurone layer, with typical contents ranging between 3-30 g kg^{-1} of rice (Kumar et al., 2023). While these are not limited to cereals but also found in pulses and legumes, they chelate with trace elements (Mg, Zn, Fe) within the intestinal lumen and can inhibit their absorption by up to 50%. However, this is a manageable limitation with treatments such as soaking (Albarracín et al., 2013), cooking (Liu et al., 2019), phytase treatment (Kumar et al., 2010) and germination (Fukushima et al., 2020), shown to significantly reduce phytic acid contents and thereby increase trace element availability. Interestingly, regular consumption of a high phytate diet has been shown to reduce the negative effects of phytates on trace element absorption (Armah et al., 2015). This may suggest that habitual long-term consumption of brown rice could at least partly negate the effects of phytates and is worthy of further study.

3.2 Distribution of micronutrient elements in rice cross-sections

Elemental maps of Cu, Mn, Fe, and Zn concentrations and distributions in 50 µm-thick brown, white, and parboiled rice samples were produced and displayed in Fig. 4(a-c). Please note that the scale/colour bar changes between these images. The scale was optimised to improve the visibility of the elements. In particular, for parboiled rice, adopting a lower concentration range was necessary to visualise the elements effectively. In general, Fig.4 shows that the abundance of these micronutrients was highest in brown rice, followed by white and parboiled rice. It can

317 be seen from the ICP-MS data (Fig. 3) that parboiled rice had the lowest
318 concentrations of these elements, which may have hampered their detection in the
319 corresponding thin sections.
320 All images show that the nutrient elements were concentrated at the grain's
321 periphery. In brown rice, this area consists of the bran (incorporating the pericarp
322 and the aleurone layer) and the sub-aleurone (outer endosperm) layer.
323 Contrastingly, in white and parboiled rice, the grain periphery consists primarily of
324 the sub-aleurone layer (and possibly small remnant quantities of the removed bran
325 layer)(Juliano & Tuaño, 2019). Most importantly, these nutrients overlapped spatially
326 in these samples. We also visualised nutrient-rich pockets or hotspots within the
327 periphery.
328 In Fig. 5, results obtained from the 150µm-thick cross-sections are presented for
329 brown (a), white (b) and parboiled (c) rice. These additional scans confirmed the
330 patterns observed in the 50µm scans, although a notable difference between the 50
331 and 150 µm-thick scans was that elements appeared more diffused around the grain
332 periphery in the latter. When the beam passes through a thicker sample, it interacts
333 with more material layers - this can have the twin effect of potentially increasing the
334 detection of certain elements while also creating a more diffused pattern.
335 There is therefore a trade-off between sample preparation for higher sensitivity
336 (thicker sections) or higher spatial resolution (thinner sections) for samples with
337 elements present in trace levels. It was apparent that the 50 µm-thick samples
338 provided a sufficiently high fluorescence signal for detecting Cu, Mn, Fe and Zn
339 concentrations in brown and white rice. In contrast, they failed to produce a
340 sufficiently strong fluorescence signal in the parboiled rice. A thicker (150 µm)
341 sample yielded a detectable signal for each measured element due to increased

342 elemental mass, making it better for parboiled rice as demonstrated in
343 Supplementary Material 3.
344 Additional scans of multiple transects located more narrowly about the edges of the
345 grain (performed on the 50 µm samples with a 30s dwell time) are presented in
346 Suppl. Material 4. These scans also confirm that these elements are concentrated in
347 the peripheral layers of the grain in comparison to the starchy interior endosperm. It
348 appears that the increased dwell time improved detection when the samples were
349 thin; however, increasing the dwell time requires vastly increased overall scanning
350 time, therefore, it is not often possible to accommodate large ROIs (e.g. full or half-
351 grain cross-sections) within the limited experimental beam time often allocated to
352 projects.
353 The nutrient element data from images strongly align with the ICP-MS results. Both
354 white and parboiled rice have a lower concentration of nutrients because the
355 nutrient-rich bran is removed during processing, unlike brown rice. However, it may
356 be noted that sXRF provides pixel-level concentration, allowing us to observe
357 heterogeneity in element distribution across the rice grain, including hotspots and
358 starchy endosperm areas free from these elements. In contrast, ICP-MS analysis
359 provides bulk grain concentration based on dried, homogenised, and acid-digested
360 samples from several rice grains.
361 Industrial production of parboiled rice involves hydrothermal treatment, comprised of
362 steeping, steaming and drying unhusked grains before milling, a treatment which is
363 believed to facilitate the diffusion of nutrient elements from bran to the endosperm of
364 the grain (Balbinoti et al., 2018). However, cooked parboiled rice images (Fig. 4c &
365 5c) show that concentrations of nutrient elements in parboiled rice were considerably
366 lower (note the differences of concentration colour maps in Figs. 4c & 5c) than in

white or brown rice, supporting the ICP-MS data (Fig. 3). The images do, however, show a diffused pattern around the edges, suggesting parboiling may enhance the diffusion of these elements into the starchy endosperm of the grain. Further studies are needed to confirm these findings, particularly data from single cultivar studies comparing raw and parboiled variants. A previous study comparing brown and processed (parboiled or polished) rice showed that most nutrient elements were reduced due to processing (Runge et al., 2019), except for Cu. However, Mn and Zn were higher in white rice than in parboiled, whereas Fe was similar. This broadly agrees with our findings. The evidence from this study and previous investigations indicates that parboiling does not enrich rice with nutrient elements.

Only a handful of studies have investigated cereals using sXRF. One study imaged longitudinal (i.e. along the long edge of the grain) sections (70 µm) of unhusked raw rice (Lombi et al., 2009) using sXRF and showed that Mn, Zn and Cu were mainly concentrated in areas in and around the embryo. In contrast, Fe was in the aleurone/pericarp region of the grain. It is worth noting that due to the polishing process involved in the production, both white and parboiled rice do not contain embryos. In our study, we utilised cooked processed rice (husked, polished, or parboiled) and prepared transverse cross-sections. Given the limited access to the sXRF facility (restricted to three days in our case), we faced a trade-off between scanning time and the area of the region of interest (ROI) to ensure reproducible results across the samples.

A recent study (Limmer et al., 2023) compared both transverse and longitudinal cross-sections of raw brown rice. The Cu, Zn and Mn concentration maps were broadly similar to our study, and Mn and Zn were strongly accumulated in the ovular vascular trace. Zn was more diffused into endosperms, although the bulk of it was

concentrated in the bran. However, their study used thinner (30 µm) cross-sections with a shorter dwell time (0.3 s). The larger beam spot size (25 µm) also means the spatial resolution was slightly lower. In contrast to Limmer et al. (2023), we avoided using epoxy resin because of the potential interferences such embedding methods can create.

It was interesting to note that we also found nutrient spatial overlap around the edge of the grain, confirming that the bulk of the nutrients were located in the bran and aleurone layers (Deng et al., 2023; Limmer et al., 2023; Lombi et al., 2009; Mihucz et al., 2010). Nutrient-rich bran and aleurone layers may not be removed entirely during polishing (white and parboiled). This results in the retention of some nutrient elements in white or parboiled rice, as illustrated in our images. Future studies could explore how varying degrees of polishing affect the nutrient element content of white or parboiled rice, since these layers contain most of these elements.

In our data, the 50 µm-thick samples generally worked well for brown and white rice but not for parboiled rice, where thicker sections were found appropriate. Ultimately, there is a compromise to be made between sensitivity and resolution for an element of interest in the sample. However, thin-sectioning cooked rice to obtain complete cross-sections without damaging the sample integrity is challenging. Nevertheless, this study confirmed that cooked brown rice was superior in nutrients to the other processed rice types used.

As part of this study, we also hoped to map other elements of interest, such as As, which is a toxin of significant concern in rice. There have been many publications on mapping As in rice (Limmer et al., 2023; Limmer & Seyfferth, 2022; Lombi et al., 2009; Meharg et al., 2008; Mihucz et al., 2010; Moore et al., 2010), but unfortunately, in the three scan settings used in this study, we were unable to obtain a sufficiently

strong signal to quantify As. This could be because the As content in the cooked rice samples was below the detection threshold of the sXRF instrument and configuration used in this study.

4.0 Conclusions

We used the microX-ray fluorescence (sXRF) beamline at the Diamond Light Source in the UK to map the spatial distribution of micronutrients (Cu, Mn, Fe and Zn) in this study. Complementary elemental analysis using ICP-MS provided bulk concentration data, with both methods yielding consistent results. Our findings indicate that brown rice contains significantly higher concentrations of these micronutrients compared to white and parboiled rice.

The sXRF imaging revealed detailed spatial distribution patterns, highlighting characteristic nutrient hotspots within grain cross-sections. Notably, these micronutrients were predominantly localised in the peripheral regions of cooked brown rice, underscoring its value as a healthier alternative to white and parboiled varieties. This information is particularly valuable for over half of the world's population, who rely on rice as their primary staple food.

Our study also provides additional insights into the effects of rice section thickness (50 and 150 µm) on sXRF sensitivity and resolution. These findings highlight important trade-offs in detection capabilities. Furthermore, sXRF imaging identified nutrient-rich pockets within the grain periphery, offering new perspectives on nutrient distribution beyond peripheral accumulation. Together, these dual-approach methodologies enhance our understanding of micronutrient localisation in cooked rice. Future studies are needed to compare different rice processing methods, such

as polishing and parboiling, and cooking methods, using rice genotypes grown under identical conditions.

Acknowledgements

We thank the Science and Technology Facility Council (STFC) Food Network+ (ST/T002921/2) for the funding. We also acknowledge Diamond Light Source for granting the beamtime on the I18 beamline under the experiment number SP34311. We also thank Ms Fiona Wright at the Medical School, University of Sheffield, for preparing the rice cross-sections for the experiment. We also thank Prof. Liz Bailey and Dr Saul V Raina for the ICP-MS analysis.

Author contributions: CRediT

Conceptualisation [MM, AS, VR, KG]; Funding acquisition [MM, AS, VR, KG]; Investigation [MM, AS, VR, KG]; Methodology [MM, AS, VR, KG, MB]; Project administration [MM, KG]; Supervision [MM]; Visualisation [KG, MB, AS, MM]; Writing – original draft [MM] and Writing – review and editing [AS, VR, KG, MB]

Reference

Adams, F. (2003). Synchrotron radiation micro-X-ray fluorescence analysis: A tool to increase accuracy in microscopic analysis. *Nuclear Instruments and Methods in Physics Research Section B: Beam Interactions with Materials and Atoms*, *199*, 375–381. https://doi.org/10.1016/S0168-583X(02)01563-X

Albarracín, M., González, R. J., & Drago, S. R. (2013). Effect of soaking process on nutrient bio-accessibility and phytic acid content of brown rice cultivar. *LWT - Food Science and Technology*, *53*(1), 76–80. https://doi.org/10.1016/J.LWT.2013.01.029

Antoine, J. M. R., Hoo Fung, L. A., Grant, C. N., Dennis, H. T., & Lalor, G. C. (2012). Dietary intake of minerals and trace elements in rice on the Jamaican market. *Journal of Food Composition and Analysis*, *26*(1–2), 111–121. https://doi.org/10.1016/j.jfca.2012.01.003

Armah, S. M., Boy, E., Chen, D., Candal, P., & Reddy, M. B. (2015). Regular consumption of a high-phytate diet reduces the inhibitory effect of phytate on nonheme-iron absorption in women with suboptimal iron stores. *Journal of Nutrition*, *145*(8), 1735–1739. https://doi.org/10.3945/jn.114.209957

Balbinoti, T. C. V., Nicolin, D. J., de Matos Jorge, L. M., & Jorge, R. M. M. (2018). Parboiled Rice and Parboiling Process. *Food Engineering Reviews 2018 10:3*, *10*(3), 165–185. https://doi.org/10.1007/S12393-018-9177-Y

Bin Rahman, A. N. M. R., & Zhang, J. (2023). Trends in rice research: 2030 and beyond. *Food and Energy Security*, *12*(2), e390. https://doi.org/10.1002/FES3.390

Cakmak, I. (2008). Enrichment of cereal grains with zinc: Agronomic or genetic biofortification? *Plant and Soil*, *302*(1–2), 1–17. https://doi.org/10.1007/S11104-007-9466-3/FIGURES/9

Chang, U. J., Hong, Y. H., Jung, E. Y., & Suh, H. J. (2014). Rice and the Glycemic Index. *Wheat and Rice in Disease Prevention and Health*, 357–363. https://doi.org/10.1016/B978-0-12-401716-0.00027-1

Deng, G., Vu, M., Korbas, M., Bondici, V. F., Karunakaran, C., Christensen, D., Bart Lardner, H. A., & Yu, P. (2023). Distribution of micronutrients in Arborg oat (Avena sativa L.) using synchrotron X-ray fluorescence imaging. *Food Chemistry*, *421*. https://doi.org/10.1016/j.foodchem.2023.135661

Dipti, S. S., Bergman, C., Indrasari, S. D., Herath, T., Hall, R., Lee, H., Habibi, F., Bassinello, P. Z., Graterol, E., Ferraz, J. P., & Fitzgerald, M. (2012). The potential of rice to offer solutions for malnutrition and chronic diseases. In *Rice* (Vol. 5, Issue 1, pp. 1–18). Springer New York LLC. https://doi.org/10.1186/1939-8433-5-16

Fukushima, A., Uchino, G., Akabane, T., Aiseki, A., Perera, I., & Hirotsu, N. (2020). Phytic Acid in Brown Rice Can Be Reduced by Increasing Soaking Temperature. *Foods*, *10*(1), 23. https://doi.org/10.3390/FOODS10010023

Goff, J. P. (2018). Invited review: Mineral absorption mechanisms, mineral interactions that affect acid–base and antioxidant status, and diet considerations to improve mineral status. *Journal of Dairy Science*, *101*(4), 2763–2813. https://doi.org/10.3168/JDS.2017-13112

Gray, P. J., Conklin, S. D., Todorov, T. I., & Kasko, S. M. (2015). Cooking rice in excess water reduces both arsenic and enriched vitamins in the cooked grain. *Food Additives and Contaminants - Part A Chemistry, Analysis, Control, Exposure and Risk Assessment*, *33*(1), 78–85. https://doi.org/10.1080/19440049.2015.1103906

International Rice Research Institute. (2013). Rice Almanac. In *GRiSP (Global Rice Science Partnership). Rice Almanac* (4th ed.).

Juliano, B. O., & Tuaño, A. P. P. (2019). Gross structure and composition of the rice grain. *Rice: Chemistry and Technology*, 31–53. https://doi.org/10.1016/B978-0-12-811508-4.00002-2

Kaur, B., Ranawana, V., & Henry, J. (2016). The Glycemic Index of Rice and Rice Products: A Review, and Table of GI Values. *Critical Reviews in Food Science and Nutrition*, *56*(2), 215–236. https://doi.org/10.1080/10408398.2012.717976

Kumar, A., Lal, M. K., Sahoo, S. K., Dash, G. K., Sahoo, U., Behera, B., Nayak, L., & Bagchi, T. B. (2023). The diversity of phytic acid content and grain processing play decisive role on minerals bioavailability in rice. *Journal of Food Composition and Analysis*, *115*, 105032. https://doi.org/10.1016/J.JFCA.2022.105032

Kumar, V., Sinha, A. K., Makkar, H. P. S., & Becker, K. (2010). Dietary roles of phytate and phytase in human nutrition: A review. *Food Chemistry*, *120*(4), 945–959. https://doi.org/10.1016/J.FOODCHEM.2009.11.052

Limmer, M. A., & Seyfferth, A. L. (2022). Altering the localization and toxicity of arsenic in rice grain. *Scientific Reports 2022 12:1*, *12*(1), 1–11. https://doi.org/10.1038/s41598-022-09236-3

Limmer, M. A., Webb, S. M., Seyfferth, A. L., & IUCr. (2023). Evaluation of quantitative synchrotron radiation micro-X-ray fluorescence in rice grain. *Urn:Issn:1600-5775*, *30*(2), 407–416. https://doi.org/10.1107/S1600577523000747

Liu, K., Zheng, J., Wang, X., & Chen, F. (2019). Effects of household cooking processes on mineral, vitamin B, and phytic acid contents and mineral bioaccessibility in rice. *Food Chemistry*, *280*, 59–64. https://doi.org/10.1016/j.foodchem.2018.12.053

Lombi, E., Scheckel, K. G., Pallon, J., Carey, A. M., Zhu, Y. G., & Meharg, A. A. (2009). Speciation and distribution of arsenic and localization of nutrients in rice grains. *New Phytologist*, *184*(1), 193–201. https://doi.org/10.1111/j.1469-8137.2009.02912.x

Mauer, V., Smalley, A., & Menon, M. (2024). Mineral nutrient elements and their bioaccessibility in hulled organic and conventional lentils (Lens culinaris) sold in the UK. *Journal of Food Composition and Analysis*, *132*. https://doi.org/10.1016/j.jfca.2024.106372

Meharg, A. A., Lombi, E., Williams, P. N., Scheckel, K. G., Feldmann, J., Raab, A., Zhu, Y., & Islam, R. (2008). Speciation and localization of arsenic in white and brown rice grains RN - Environ. Sci.Technol. 42, 1051-1057. *Environmental Science & Technology*, *42*(4), 1051–1057. https://doi.org/10.1021/es702212p

Menon, M., Dong, W., Chen, X., Hufton, J., & Rhodes, E. J. (2021). Improved rice cooking approach to maximise arsenic removal while preserving nutrient elements. *Science of the Total Environment*, *755*, 143341. https://doi.org/10.1016/j.scitotenv.2020.143341

Menon, M., Nicholls, A., Smalley, A., & Rhodes, E. (2024). A comparison of the effects of two cooking methods on arsenic species and nutrient elements in rice. *Science of the Total Environment*, *914*. https://doi.org/10.1016/j.scitotenv.2023.169653

Menon, M., Sarkar, B., Young, S., Hufton, J., Reynolds, C., Reina, S. V., & Young, S. (2020). Do arsenic levels in rice pose a health risk to the UK population ? *Ecotoxicology and Environmental Safety*, *197*(January), 110601. https://doi.org/10.1016/j.ecoenv.2020.110601

Menon, M., Smith, A., & Fennell, J. (2022). Essential nutrient element profiles in rice types: A risk-benefit assessment including inorganic arsenic. *British Journal of Nutrition*, *128*(5), 888–899. https://doi.org/10.1017/S0007114521004025

Mihucz, V. G., Silversmit, G., Szalóki, I., Samber, B. de, Schoonjans, T., Tatár, E., Vincze, L., Virág, I., Yao, J., & Záray, G. (2010). Removal of some elements from washed and

cooked rice studied by inductively coupled plasma mass spectrometry and synchrotron based confocal micro-X-ray fluorescence. *Food Chemistry*, *121*(1), 290–297. https://doi.org/10.1016/j.foodchem.2009.11.090

Moore, K. L., Schröder, M., Lombi, E., Zhao, F.-J. J., McGrath, S. P., Hawkesford, M. J., Shewry, P. R., & Grovenor, C. R. M. M. (2010). NanoSIMS analysis of arsenic and selenium in cereal grain. *New Phytologist*, *185*(2), 434–445. https://doi.org/10.1111/j.1469-8137.2009.03071.x

Mosselmans, J. F. W., Quinn, P. D., Dent, A. J., Cavill, S. A., Moreno, S. D., Peach, A., Leicester, P. J., Keylock, S. J., Gregory, S. R., Atkinson, K. D., & Rosell, J. R. (2009). I18 – the microfocus spectroscopy beamline at the Diamond Light Source. *Urn:Issn:0909-0495*, *16*(6), 818–824. https://doi.org/10.1107/S0909049509032282

Nealon, N. J., Parker, K. D., Lahaie, P., Ibrahim, H., Maurya, A. K., Raina, K., & Ryan, E. P. (2019). Bifidobacterium longum-fermented rice bran and rice bran supplementation affects the gut microbiome and metabolome. *Beneficial Microbes*, *10*(8), 823–839. https://doi.org/10.3920/BM2019.0017

Oli, P., Ward, R., Adhikari, B., Mawson, A. J., Adhikari, R., Wess, T., Pallas, L., Spiers, K., Paterson, D., & Torley, P. (2016). Synchrotron X-ray Fluorescence Microscopy study of the diffusion of iron, manganese, potassium and zinc in parboiled rice kernels. *LWT - Food Science and Technology*, *71*, 138–148. https://doi.org/10.1016/J.LWT.2016.03.034

Pinto, E., Almeida, A., & Ferreira, I. M. P. L. V. O. (2016). Essential and non-essential/toxic elements in rice available in the Portuguese and Spanish markets. *Journal of Food Composition and Analysis*, *48*, 81–87. https://doi.org/10.1016/j.jfca.2016.02.008

Runge, J., Heringer, O. A., Ribeiro, J. S., & Biazati, L. B. (2019). Multi-element rice grains analysis by ICP OES and classification by processing types. *Food Chemistry*, *271*(July 2018), 419–424. https://doi.org/10.1016/j.foodchem.2018.07.162

Saleh, A. S. M., Wang, P., Wang, N., Yang, L., & Xiao, Z. (2019). Brown Rice Versus White Rice: Nutritional Quality, Potential Health Benefits, Development of Food Products, and Preservation Technologies. *Comprehensive Reviews in Food Science and Food Safety*, *18*(4), 1070–1096. https://doi.org/10.1111/1541-4337.12449

Shi, Z., Carey, M., Meharg, C., Williams, P. N., Signes-Pastor, A. J., Triwardhani, E. A., Pandiangan, F. I., Campbell, K., Elliott, C., Marwa, E. M., Jiujin, X., Farias, J. G., Nicoloso, F. T., De Silva, P. M. C. S., Lu, Y., Norton, G., Adomako, E., Green, A. J., Moreno-Jiménez, E., … Meharg, A. A. (2020). Rice Grain Cadmium Concentrations in the Global Supply-Chain. *Exposure and Health*, *12*(4), 869–876. https://doi.org/10.1007/S12403-020-00349-6/FIGURES/4

Solé, V. A., Papillon, E., Cotte, M., Walter, P., & Susini, J. (2007). A multiplatform code for the analysis of energy-dispersive X-ray fluorescence spectra. *Spectrochimica Acta Part B: Atomic Spectroscopy*, *62*(1), 63–68. https://doi.org/10.1016/J.SAB.2006.12.002

Stevens, G. A., Beal, T., Mbuya, M. N. N., Luo, H., Neufeld, L. M., Addo, O. Y., Adu-Afarwuah, S., Alayón, S., Bhutta, Z., Brown, K. H., Jefferds, M. E., Engle-Stone, R., Fawzi, W., Hess, S. Y., Johnston, R., Katz, J., Krasevec, J., McDonald, C. M., Mei, Z., … Young, M. F. (2022). Micronutrient deficiencies among preschool-aged children and women of reproductive age worldwide: a pooled analysis of individual-level data from population-representative surveys. *The Lancet Global Health*, *10*(11), e1590–e1599. https://doi.org/10.1016/S2214-109X(22)00367-9

Wang, C., Lu, Y., Wang, J., & Zhong, C. (2022). The sub-cellular distribution of Zn and trace elements in the wheat grain: in situ imaging using a NanoSIMS. *Cereal Research*

Communications, *50*(4), 1127–1135. https://doi.org/10.1007/S42976-022-00269-Y/TABLES/1

Welch, R. M., & Graham, R. D. (2004). Breeding for micronutrients in staple food crops from a human nutrition perspective. *Journal of Experimental Botany*, *55*(396), 353–364. https://doi.org/10.1093/jxb/erh064

Welch, R. M., & Graham, R. D. (2005). Agriculture: The real nexus for enhancing bioavailable micronutrients in food crops. *Journal of Trace Elements in Medicine and Biology*, *18*(4), 299–307. https://doi.org/10.1016/j.jtemb.2005.03.001

White, P. J., & Broadley, M. R. (2009). Biofortification of crops with seven mineral elements often lacking in human diets – iron, zinc, copper, calcium, magnesium, selenium and iodine. *New Phytologist*, *182*(1), 49–84. https://doi.org/10.1111/J.1469-8137.2008.02738.X

Williams, P. N., Villada, A., Deacon, C., Raab, A., Figuerola, J., Green, A. J., Feldmann, J., & Meharg, A. A. (2007). Greatly enhanced arsenic shoot assimilation in rice leads to elevated grain levels compared to wheat and barley. *Environmental Science and Technology*. https://doi.org/10.1021/es070627i

Wu, X., Guo, T., Luo, F., & Lin, Q. (2023). Brown rice: a missing nutrient-rich health food. *Food Science and Human Wellness*, *12*(5), 1458–1470. https://doi.org/10.1016/J.FSHW.2023.02.010

Yilmaz, B., & Li, H. (2018). Gut Microbiota and Iron: The Crucial Actors in Health and Disease. *Pharmaceuticals 2018, Vol. 11, Page 98*, *11*(4), 98. https://doi.org/10.3390/PH11040098

647 **Figure captions**

648

649 Fig 1. A schematic representation of brown rice grain with different layers (a) and screenshot
650 images of brown (b), white (c) and parboiled (d) cross-sections mounted for imaging.
651 Fig 2: Representative sXRF spectrum from one pixel of a brown rice segment fitted in
652 PyMca. The black line represents the raw data, the green line represents the background
653 continuum, and the red line shows the fitted data incorporating the peaks of the elements
654 identified.
655 Figure 3. The mean concentrations of nutrient elements (Cu, Mn, Fe and Zn) in white,
656 parboiled and brown rice samples based on ICP-MS analysis. The error bars represent the
657 standard deviation of the mean.
658 Figure 4. The distribution of Cu, Mn, Fe and Zn concentrations in different brown, white and
659 parboiled cross sections (50µm) quantified using PyMca. Please note the differences in
660 scale and dimensions in these panels.
661 Figure 5. The distribution of Cu, Mn, Fe and Zn concentrations in different brown, white and
662 parboiled cross sections (150µm) quantified using PyMca. Please note the differences in
663 scale and dimensions in these panels.

(a)

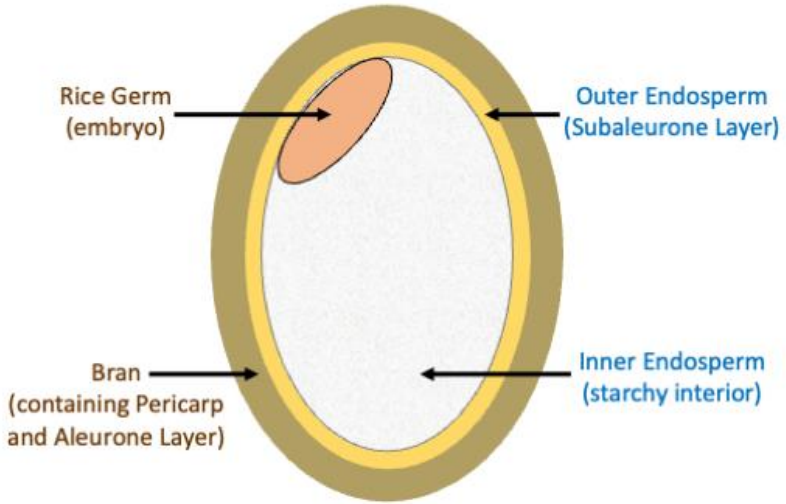

(b)

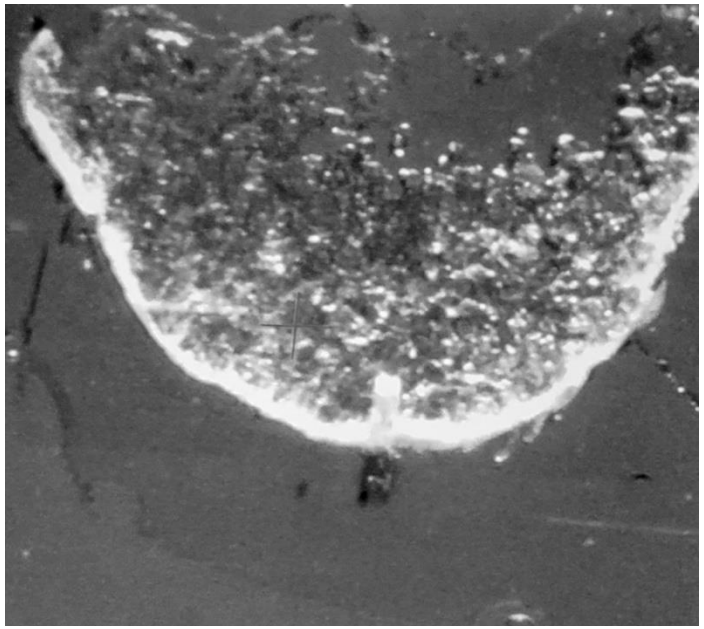

(c)

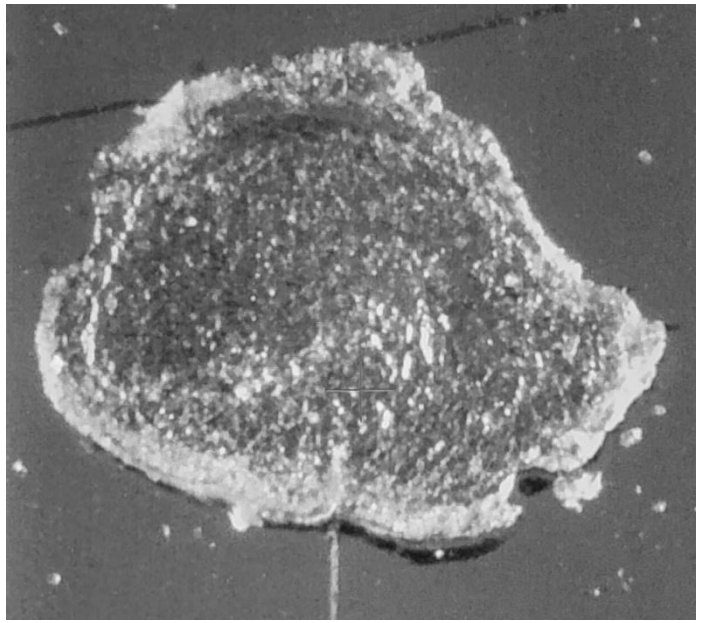

(d)

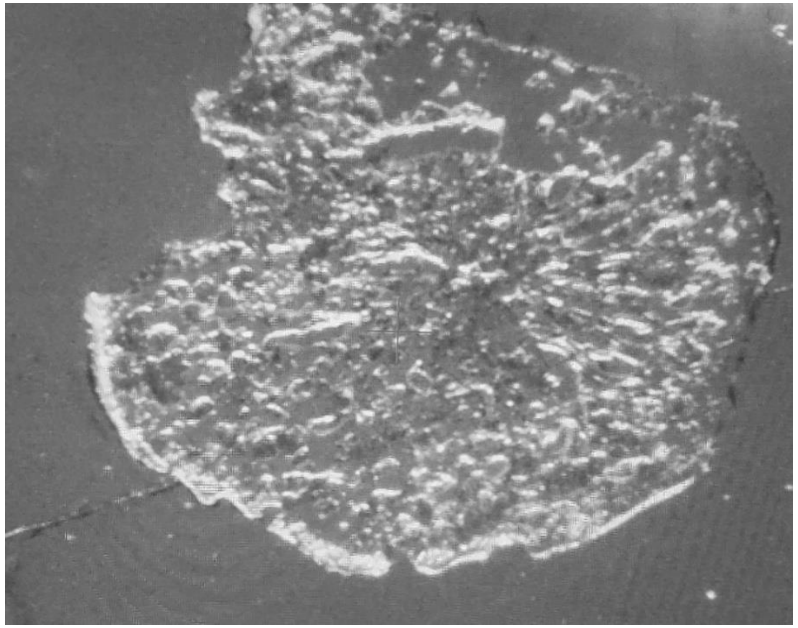

Figure 1

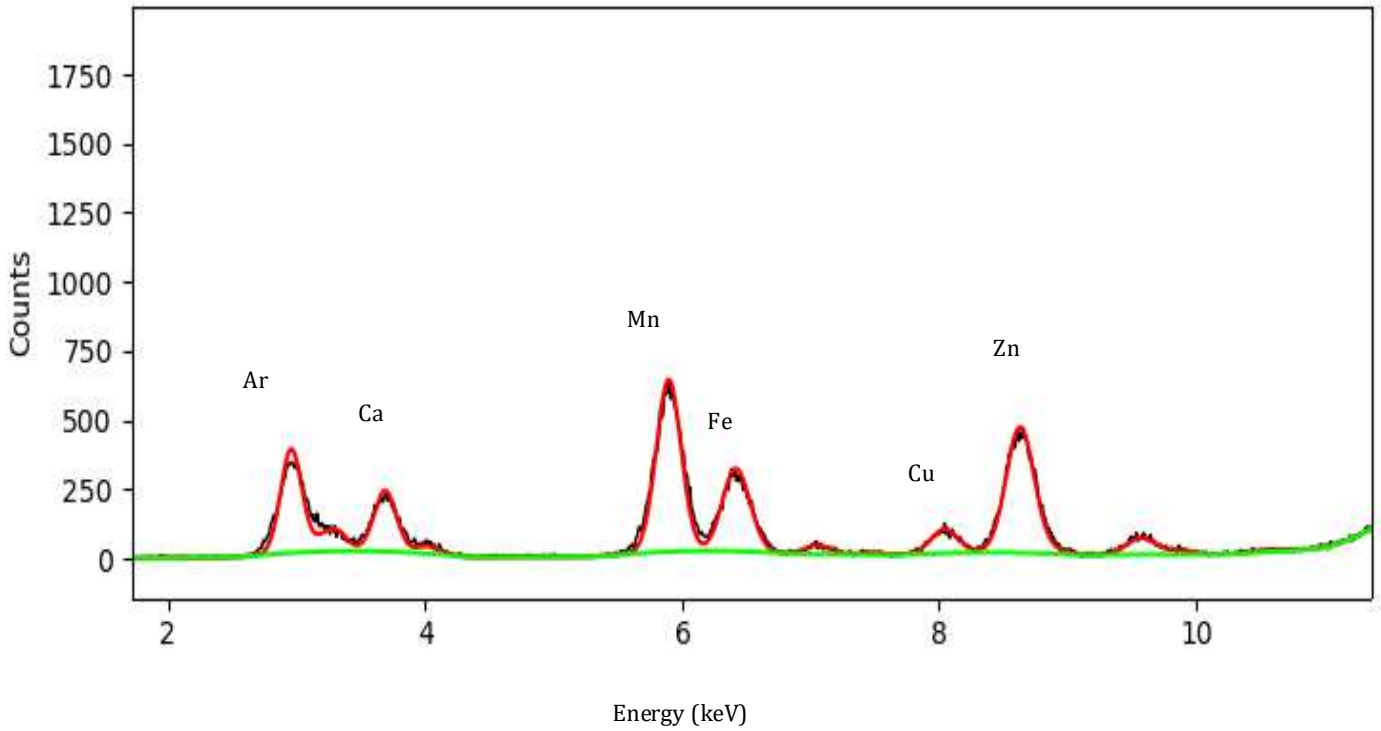
1750
1500
1250
1000
750
500
250
0
Counts
Ar
Ca
Mn
Fe
Cu
Zn
2
4
6
8
10
Energy (keV)

Figure 2

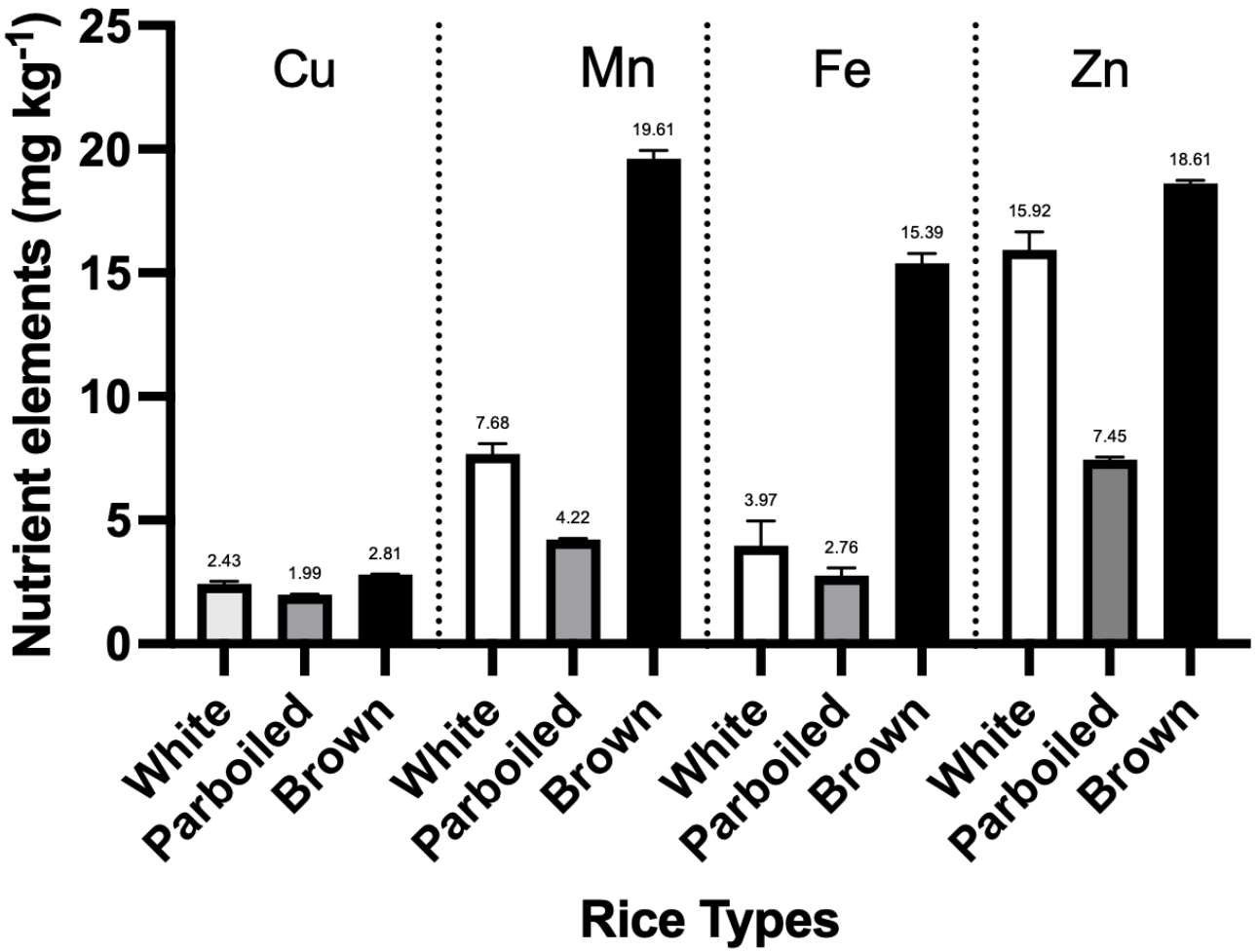
Nutrient elements (mg kg-1)
25
20
15
10
5
0
Cu
Mn
Fe
Zn
2.43
1.99
2.81
7.68
4.22
19.61
3.97
2.76
15.39
15.92
7.45
18.61
White
Parboiled
Brown
White
Parboiled
Brown
White
Parboiled
Brown
White
Parboiled
Brown
Rice Types

Figure 3

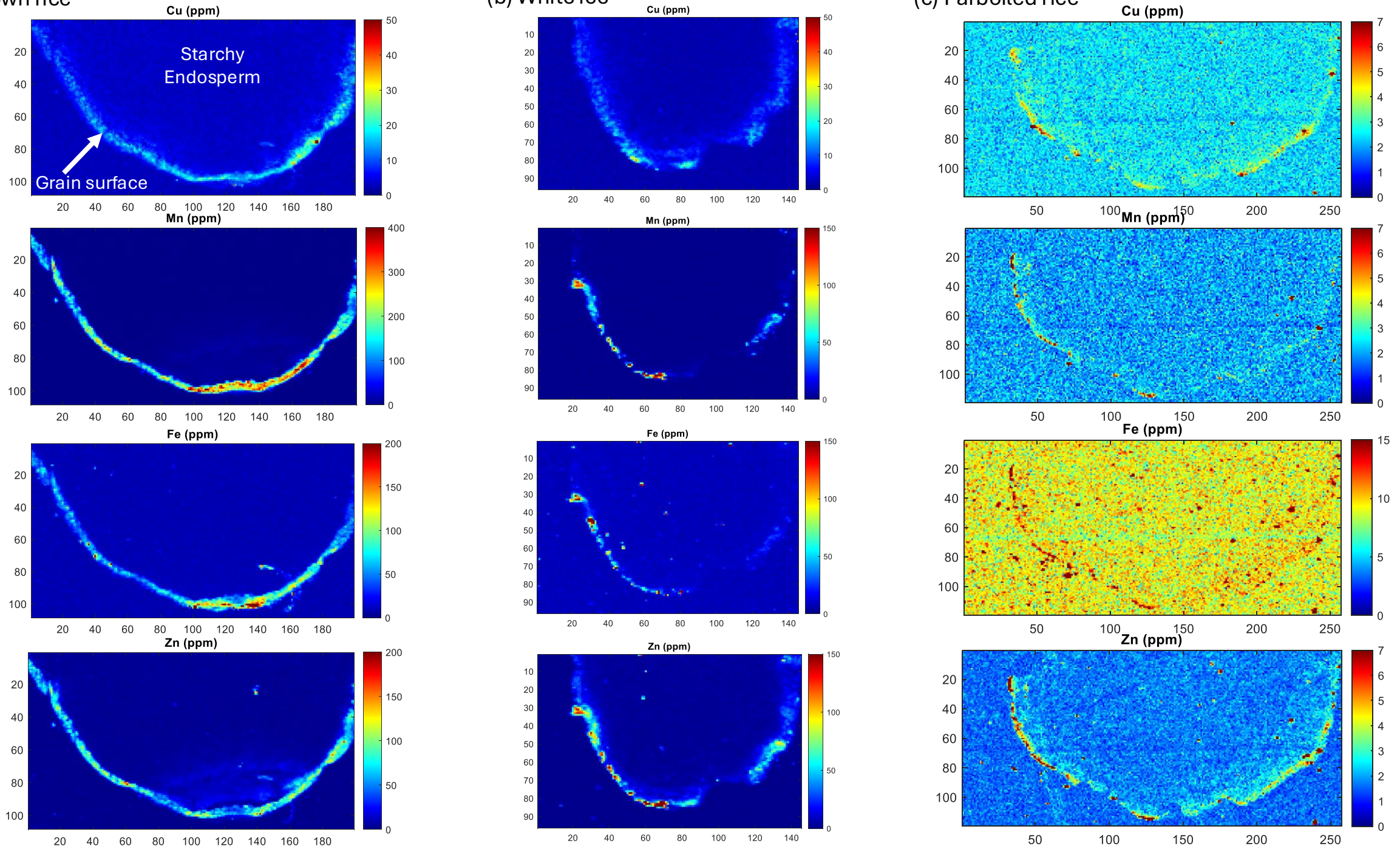
(a) Brown rice
(b) White ice
(c) Parboiled rice
Cu (ppm)
Mn (ppm)
Fe (ppm)
Zn (ppm)
Starchy
Endosperm
Grain surface

Figure 4

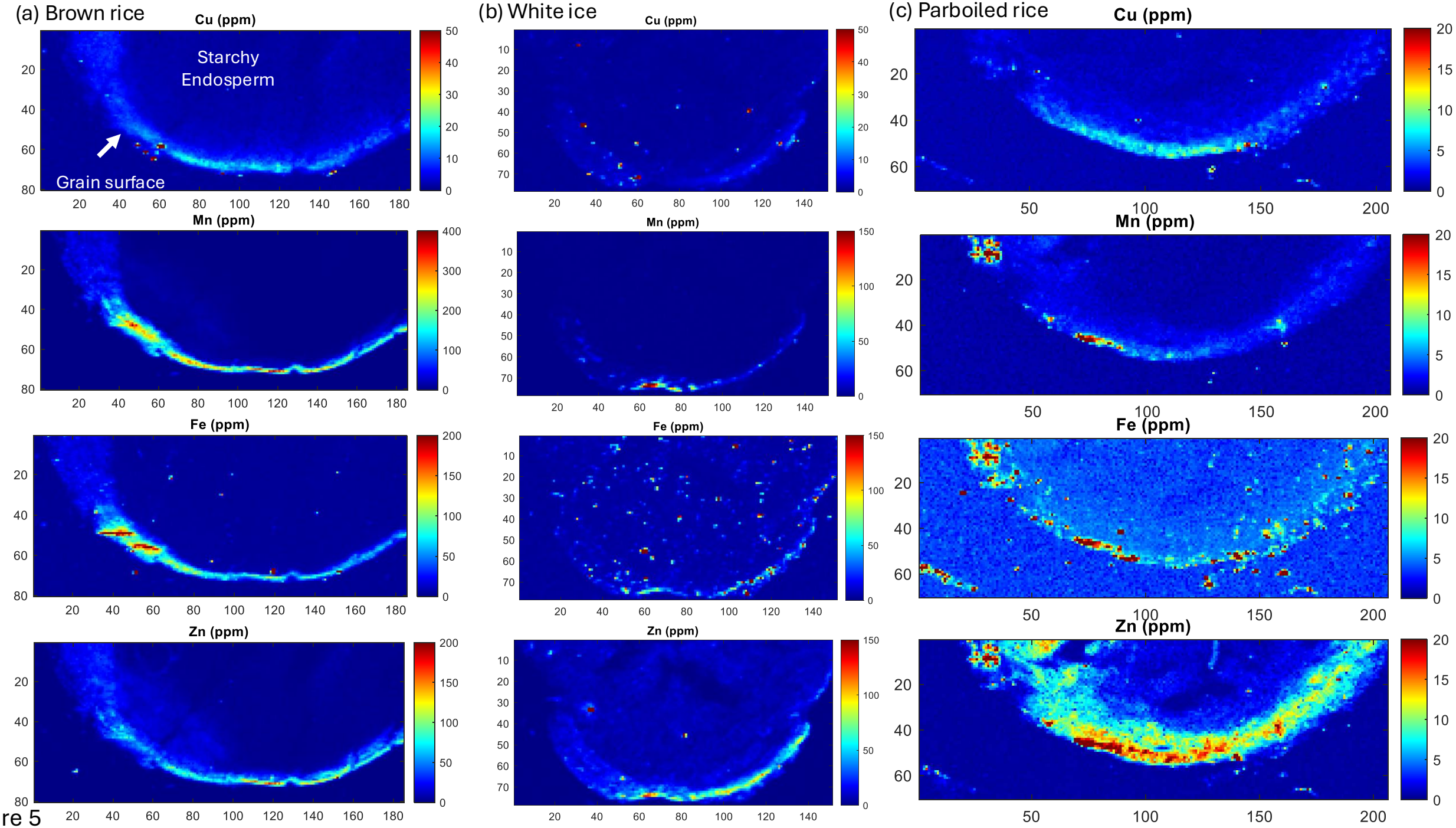
(a) Brown rice
(b) White ice
(c) Parboiled rice
Cu (ppm)
Mn (ppm)
Fe (ppm)
Zn (ppm)
Starchy
Endosperm
Grain surface

Figure 5

Declaration of interests

☒ The authors declare that they have no known competing financial interests or personal relationships that could have appeared to influence the work reported in this paper.

☐The authors declare the following financial interests/personal relationships which may be considered as potential competing interests: